This paper was published in ACI SP-123 Design of Beam-Column Joints for Seismic Resistance, James O. Jirsa Editor, American Concrete Institute, Michigan, 1991, pp. 97 - 123.

DEVELOPMENT OF DESIGN CRITERIA FOR RC INTERIOR BEAM-COLUMN JOINTS

Kazuhiro KITAYAMA, Shunsuke OTANI and Hiroyuki AOYAMA

Synopsis: A series of research efforts, at the University of Tokyo, leading to the development of earthquake resistant design criteria for reinforced concrete interior beam-column joints are briefly summarized. The design criteria emphasize the protection of the joint to an acceptable deformation level of a frame structure during an intense earthquake. For the design against shear, shear resisting mechanism by truss and concrete compression strut, the role of joint lateral reinforcement, and the effect of transverse beams and slabs were studied experimentally. The requirement for beam bar bond was discussed on the basis of nonlinear earthquake response analysis.

Keywords: Beams (supports); bond (concrete to reinforcement t); columns (supports); deformation; earthquake resistant structures; joints (junctions); reinforced concrete; shear properties; structural design

Dr. K. Kitayama, graduate of University of Tokyo, is a research associate of Architecture at Utsunomiya University, Tochigi. He studies the behavior and earthquake resistant design of reinforced concrete beam-column joints.

Dr. S. Otani, graduate of University of Tokyo and University of Illinois at Urbana-Champaign, is an associate professor of Architecture at the University of Tokyo. He was awarded with the 1990 Architectural Institute of Japan Research Award for his work on Nonlinear Earthquake Response Analysis of Reinforced Concrete Buildings.

Dr. H. Aoyama, ACI Fellow, graduate of University of Tokyo, is a professor of Architecture at the University of Tokyo. He is the recipient of the 1977 Architectural Institute of Japan Research Award for his work on Earthquake Resistance of Reinforced Concrete Structures.

INTRODUCTION

A reinforced concrete (R/C) building in Japan has traditionally been designed for a large earthquake load, which normally resulted in wide columns. Hence, the damage by shear and beam bar slippage within a beam-column joint was scarcely observed in the past earthquakes. However, the advancement of design calculation and the use of higher strength materials might reduce column dimensions, especially with the adoption of an ultimate strength design procedure

relying on the ductility. Then, the beam-column joint may become the weak link of a chain, which necessitated a serious examination of the joint design in Japan.

A heavy damage in a beam-column joint should beam voided during an earthquake because (a) the gravity load is sustained by the joint, (b) a large ductility and energy dissipation is hard to achieve in the joint, and (c) a joint is difficult to repair after an earthquake. However, an excessive complication of reinforcement detailing should be equally avoided to insure good workmanship and construction. Therefore, joint shear failure and a significant beam bar slippage within a joint should be prevented up to an expected structural deformation, which this paper arbitrarily assumes to be "a beam ductility factor of 4" or "a story drift angle of 1/50 rad," whichever is smaller.

A remarkable difference exists in the seismic design provisions for beam-column joints between New Zealand NZS 3101:1982 (Ref. 1) and the U.S ACI code (Ref. 2). NZS 3101 requires a large amount of lateral reinforcement in a joint to resist a dominant part of the joint shear by the truss mechanism, relying on the good bond stress transfer along the longitudinal reinforcement, while ACI code assumes the diagonal compression concrete strut to resist the shear. The use of larger-diameter and higher-strength bars for beam flexural reinforcement is limited in NZS 3101 to reduce the bar slippage within the joint.

This paper discusses the influence of beam bar bond deterioration within a joint on earthquake response of R/C frame structures, joint shear transfer mechanisms, the role of joint lateral reinforcement, and the effect of framing members on the joint shear strength.

SHEAR RESISTING MECHANISMS OF BEAM-COLUMN JOINT

Paulay et al. (Ref. 3) proposed shear transfer mechanisms of a joint, as shown in Fig. 1, called "a diagonal strut mechanism" and "a truss mechanism." The diagonal compression strut is formed along the main diagonal of a joint panel by the resultant of the horizontal and vertical compression stresses and shear stresses acting on the concrete at the beam and column critical sections. The truss mechanism is formed with uniformly distributed diagonal compression stresses, tensile stresses in the vertical and horizontal reinforcement and the bond stresses acting along the beam and column exterior bars.

The results of two series of half scale planar interior beam-column sub-assemblage tests (called J- and C-series) are compared to study the joint shear transfer mechanisms (Refs. 4, 5). The properties of Specimens J1 and C1 are summarized in Table 1. The overall dimensions were common in the two series. The loading method is shown in Fig. 2. Note that the tensile

reinforcement ratio of the specimens was quite large compared to that commonly used in a frame structure because the specimens were designed to develop high shear stresses in the joint after beam yielding. However, the amount of the beam top reinforcement in the C-series specimens was limited by the bar spacing requirements. The bond stress transfer along the beam reinforcement is expected to be more critical in J-series specimens, while the bond situation was improved in C-series specimens by using lower strength and smaller diameter beam bars.

Crack patterns of Specimens J1 and C1 are compared in Fig. 3 at the end of the tests. As expected, Specimen J1 failed in shear in the joint at a story drift angle of 1/23, when the shell concrete spalled off. Specimen C1 could maintain the joint panel to the end of the test and developed an ideal beam flexural hinging at the beam ends. The number of diagonal shear cracks was less in Specimen J1, and X-shaped cracks gradually opened along the main diagonal of the joint panel with deformation. Specimen C1 developed many fine diagonal cracks uniformly distributed over the joint panel. The story shear-story drift relations are compared for Specimens J1 and C1 in Fig. 4. Specimen J1 exhibited pinching hysteretic shape especially after a story drift angle of 1/46, while Specimen C1 developed good spindle shape hysteresis. It should be pointed out, however, that the joint shear stress developed in Specimen J1 was approximately 1.25 times larger than that in Specimen C1.

The crack pattern in the joint support the concept of the diagonal strut and truss mechanism associated with good and poor bonding along the beam reinforcement. Note that Specimen J1 developed shear cracks initially caused by the truss mechanism, but the shear cracks in the main diagonal became dominant at a large deformation; i.e., the truss mechanism was lost with the bond deterioration along the beam reinforcement, and the principal stress concentrated along the main diagonal strut to cause shear failure. On the other hand, the diagonal strut and truss mechanisms were maintained in Specimen C1 and diagonal compression stresses distributed uniformly in the panel concrete.

Note that the diagonal strut mechanism can exist without any bond stress transfer along the beam and column reinforcement within the joint, while the truss mechanism can develop only when good bond stress transfer is maintained along the beam and column reinforcement. It should be pointed out that the bond along the beam reinforcement inevitably deteriorates especially after the beam flexural yielding unless the strength and size of the reinforcement are strictly restricted. With the bond deterioration, the truss mechanism starts to diminish and the diagonal strut mechanism must resist dominant part of the joint shear. Note that the tension force of the beam reinforcement, not transferred to the joint concrete by the bond, must be resisted by the concrete at the compression face of the joint, increasing the magnitude of compression stresses in the main strut. Because the strut concrete is weakened by the reversed cyclic loading and because the compressive strength is reduced by the increasing tensile strain perpendicular to the direction

of the main diagonal strut, the shear capacity of the main strut decreases and eventually fails in shear compression. The principal role of the lateral reinforcement in this case is to confine the cracked joint core concrete.

EFFECT OF BOND DETERIORATION ON EARTH QUAKE RESPONSE

The bond deterioration of beam bars within a joint is said to be undesirable because (a) the energy dissipation at beam ends is reduced by pinching in a hysteresis shape, (b) the diagonal compressive stresses increase with a change in the joint shear transfer mechanism after beam yielding, and (c) the beam deformation increases due to the bar slip within a joint. The influence of the energy dissipation capability at the beam ends on earthquake response is studied to discuss the permissibility of the beam bar slip within a joint.

The earthquake response analyses were carried out on 4-, 7- and 16-story moment-resisting frames with a 6.0 m span and uniform story height of 3.5 m. The buildings were designed in accordance with Japanese Building Standard Law, and to form a weak beam-strong column frame structure. Total height, total weight, fundamental period and design base shear coefficient are listed in Table 2, and the member dimensions in Table 3. The mass of each floor was estimated on the basis of member dimensions and floor slab thickness of 130 mm.

A part of building (a fish-bone model, Fig. 5), consisting of a continuous column and beams connected on both sides of the column, was removed from the proto type building by cutting beams at the inflection point located at the beam mid span (Ref. 6). The beam and column member were represented by one component model, in which inelastic deformation of a member was assumed to concentrate in the nonlinear spring. Beam-column joints were assumed to be rigid.

The hysteresis models at beam ends were selected to simulate the pinching behavior caused by the bond deterioration along the beam reinforcement (Takeda Slip hysteresis model). Takeda model was used to simulate a good bond situation with a spindle-shape hysteresis (Fig. 6). The skeleton curves of both models were common. An equivalent viscous damping ratio h_{eq}, ratio of the dissipated energy within half a cycle to 2π times the strain energy at peak of an equivalent linearly elastic system, was 0.25 for Takeda model, and 0.15 and 0.10 for Takeda-Slip models at a ductility factor of 4.0. The additional deformation caused by the pull-out of beam bars from a joint was not considered in the analysis.

Viscous damping matrix was assumed to be proportional to instantaneous stiffness matrix, and the initial elastic damping factor for the first mode was chosen to be 0.05 of the critical. Input

earthquake motions were the 1940 El Centro (NS) record and the 1952 Taft (S69E) record. The intensity of ground motions was adjusted to develop maximum member ductility factors of approximately 4.0 at beam ends in the structures using the Takeda model. Note that the design story drift is normally exceeded under this response.

The attained ductility factors at beam ends are shown in Fig. 7. The distribution of beam-end ductility factors of structure with the Takeda model is similar to that with the Takeda-Slip model (h_{eq}=0.15). The change in the h_{eq} value of the Takeda-Slip model from 0.15 to 0.10 did not affect the ductility demand appreciably. The maximum drift was comparable for the three structures, although the large drift developed more frequently in the structure with the Takeda-Slip models.

It was concluded that the effect of hysteresis energy dissipation capacity on the response amplitude was relatively small for a range of equivalent viscous damping ratio from 0.10 to 0.25 at a ductility factor of 4.0. Therefore, some bond deterioration of beam bars within a joint may be tolerable.

LIMITATION OF BEAM M BAR BOND INDEX

A beam bar bond index was introduced to indicate the severity of bond stress relative to the bond strength. A maximum bond stress u_b of beam reinforcement over the column width was estimated by assuming simultaneous yielding of the beam reinforcement in tension and compression at the two faces of the joint. The bond strength was assumed proportional to the square root of the concrete compressive strength. The beam bar bond index BI was defined by dividing the average bond stress by the square root of the concrete strength (Ref. 6);

$$\frac{u_b}{\sqrt{f_c'}} = \frac{f_y}{2\sqrt{f_c'}} \frac{d_b}{h_c} \qquad (1)$$

where f_y: yield strength of beam bars in kgf/cm^2, d_b: diameter of beam bars, h_c: column width and f_c': concrete compressive strength in kgf/cm^2.

The beam bar bond index $u_b / \sqrt{f_c'}$ and the equivalent viscous damping ratio h_{eq} at a story drift angle of 1/50 rad are compared for the plane beam-column joints tested previously in Japan (Fig. 8). The solid line was derived from the least squares method to fit the data. Concrete compressive strength was greater than 270 kgf/cm^2 for specimens with open symbols. The values of h_{eq} decrease with an increasing $u_b / \sqrt{f_c'}$ value. If an allowable deformation level is taken

to be a story drift angle of 1/50 rad, the $u_b / \sqrt{f_c'}$ value should satisfy Eq. (2) to ensure the equivalent viscous damping ratio of 0.10;

$$\frac{u_b}{\sqrt{f_c'}} \leq 4.5 \tag{2}$$

Substituting u_b in Eq. (1) into Eq. (2),

$$\frac{h_c}{d_b} \geq \frac{f_y}{9\sqrt{f_c'}} \tag{3}$$

a design requirement for column width-beam bar diameter relation is proposed.

ROLE OF JOINT LATERAL REINFORCEMENT

Three half-scale planar interior beam-column joint specimens (Specimens B1, B2 and B3) were tested varying reinforcement detailing and amount in a joint (Ref. 7). The role of the lateral reinforcement was studied; i.e., lateral reinforcement to resist shear and that to confine core concrete. Also studied was the amount of joint lateral reinforcement required to confine joint core concrete after bond deterioration along the beam reinforcement and at high joint shear. The member dimensions were common in the three specimens. Beam sections were 200x300 mm and column sections were 300x300 mm. Specimens were designed to develop a shear as high as approximately 0.3 f_c' at beam flexural yielding, where f_c' is the concrete strength. The beam bar bond indices were 5.20 for Specimens B1 and B2, and 3.33 for Specimen B3.

The specimen properties are listed in Table 1 and Fig. 9. Legged ties were used in the two orthogonal directions in Specimens B1 and B3. Ties parallel to loading direction, indicated by circle 1 in Figs. 9.a and 9.c, would resist joint shear by the truss mechanisms and confine joint core concrete in that direction, whereas transverse ties, indicated by circle 2, would restrain the expansion of core concrete normal to the loading direction. Usual closed hoops were placed in specimen B2, which would resist shear and also confine the core concrete. Note that the portions in a closed hoop parallel and normal to the loading direction influence each other. Joint lateral reinforcement ratios were 0.35 % in specimens B1 and B2, and 0.88 % in Specimen B3.

The top of the column was loaded by two actuators(Fig. 2); the one applied reversing horizontal load and the other constant vertical load. The beam ends were supported by horizontal rollers, while the bottom of the column was supported by mechanical hinge.

The joints did not fail in shear up to a story drift angle of 1/50 rad although the joint shear stress reached as high as $0.31 f_c'$ in Specimens B1 and B2, and $0.28 f_c'$ in Specimen B3. The effective joint area to resist shear is defined by the column depth and the average of the beam and column widths.

Approximately 40 % of the total story drift was caused by the joint shear deformation, comparable to the beam deflections, in the three specimens. The damage, however, came to concentrate in the joint panel region due to high shear after a story drift angle of 1/25 rad. Pinched hysteresis shape (Fig. 10) was caused by both shear distress in the joint core concrete and bond deterioration along the beam bars.

The sum of the bond forces along the beam reinforcement within a joint, which represents the part of joint shear, is shown in Fig. 11. The bond stress was evaluated as the difference in reinforcing bar stresses at the two faces of the joint. The bond forces in Specimens B1 and B3 started to decrease at a story drift angle greater than 1/100 rad, but before yielding in the beam reinforcement.

The joint legged ties in the loading direction resisted shear and also confined core concrete, as deformation increased in Specimens B1 and B3 (Fig. 12) to a story drift angle of 1/100 rad forming the truss mechanism. The strains, however, did not change appreciably at a story drift angle from 1/100 rad to 1/50 rad, at amplitudes less than the yielding strain. The strain distribution and amplitudes in Specimens B1 and B3 were similar although the amount of joint lateral reinforcement was significantly different in the two specimens. On the other hand, strains in the joint legged ties normal to the loading direction in Specimen B1 and B3, for confinement effect, increased with deformation (Figs. 13.a and 13.c).

The sum of the forces in the joint legged reinforcement, parallel and normal to the loading directions, is shown in Fig. 14 for SpecimensB1 and B3. Note that the difference in forces in the legged ties parallel and orthogonal to the loading direction, shown as shaded area in Fig. 14, indicates the joint shear carried by the lateral reinforcement. The contribution of joint lateral reinforcement to shear resistance by the truss mechanism decayed after a story drift angle of 1/100 rad, corresponding to the bond deterioration along the beam longitudinal bars, and the principal role of joint lateral reinforcement came to confine the cracked joint core concrete. Half of lateral reinforcement in the joint in Specimens B1 and B3 carried shear at a story drift angle of approximately 1/100 rad.

Strains in the lateral reinforcement normal to the loading direction is Specimens B1 and B2 increased with story drift (Fig. 13.a and 13.b) attributable to the expansion of the core concrete, but the strains did not reach the yield value before a story drift angle of 1/50 rad. Therefore, a

lateral reinforcement ratio of less than 0.35% may be sufficient to confine the joint core concrete.

EFFECT OF TRANSVERSE BEAMS ON JOINT SHEAR STRENGTH

Unloaded transverse beams can enhance joint shear resistance apparently because of the increase in effective volume of the joint. However, with development of wide flexural cracks at the column faces over the entire cross section, the beneficial effect of the transverse beams was expected to disappear. Therefore, three dimensional interior beam-column joint specimens with transverse beams (Specimen A2 without slabs and Specimen A3 with slabs) were tested (Ref. 8). Interior beam-column joint Specimens A1 (without slabs) and A4 (with slabs) without transverse beams were also tested for comparison. The properties of the specimens are listed in Table 4 and the material properties in Table 5.

The dimensions of beams and columns were identical to those of B-series specimens. The thickness of slabs was 70 mm. The specimens were designed to develop shear compression failure in the joint core concrete by using the large amount of beam reinforcing bars of high strength. The top tensile reinforcement ratio in Specimens A1 and A2 beam was 2.05 %, but less than the balanced reinforcement ratio (2.45 %) considering compressive reinforcement. The amount of beam top bars in Specimens A3 and A4 with slabs was decreased because the entire slab reinforcement may contribute to the beam flexural resistance. The shear stress level was approximately $0.4 f_c'$ at beam flexural yielding. The beam bar bond index $u_b / \sqrt{f_c'}$ was as high as 9.53. The amount of transverse beam reinforcement in Specimens A2 and A3 was determined to limit the joint shear stress to $0.2 f_c'$ in order to prevent severe damage in a joint core concrete during the transverse loading. Joint lateral reinforcement of 0.37%, which was expected sufficient to confine the joint core, was placed in all specimens.

Specimens were loaded at the top of the column, supporting the beam ends by horizontal rollers. The transverse beams were initially loaded cyclically to flexural yielding and then the longitudinal beams were tested under reversed loading.

Story drift-joint shear stress relation normalized by the concrete compressive strength f_c' are shown in Fig. 15. The effective joint area to resist shear is defined by the column depth and the average of the beam and column widths. Specimens A2 and A3 with loaded transverse beams developed beam flexural yielding and did not fail in joint shear even at a story drift angle of 1/15 rad. The maximum joint shear stress in Specimens A2 and A3 was as high as $0.36 f_c'$ and $0.40 f_c'$, respectively, but the input shear was limited by the beam flexural yielding. On the contrary, Specimens A1 and A4 without transverse beams failed in diagonal compression of the joint core concrete, develop ping the joint shear strength of $0.30 f_c'$ and $0.33 f_c'$, respectively.

Note that the transverse beam, even loaded to flexural yielding, could enhance the joint shear strength at least 1.2 times more than that without the transverse beams.

Strains along a reinforcing bar in the transverse beams in Specimen A2 during the longitudinal loading are shown in Fig. 16. The strains within and near the joint increased with story drift, and reached the yield value at a story drift angle greater than 1/25 rad although these transverse beams were not loaded during the longitudinal loading. The compressive reaction to the tensile force in the transverse beam reinforcement must have confined the joint core concrete laterally (Fig. 17). If the flexural cracks open too wide at the column faces of the transverse beams, however, such confinement action may not develop. Average flexural crack width at the critical section of the transverse beams was approximately 0.4 mm in Specimens A2 and A3.

Therefore, the shear strength of a joint will increase with the existence of transverse beams despite loading to flexural yielding. The increase is attributed to the confinement by the longitudinal reinforcement in the transverse beams. The confining effect may be directly related to the amount of the tensile reinforcement.

EFFECT OF FLOOR SLABS ON JOINT SHEAR STRENGTH

The influence of floor slabs on the shear strength of interior joints can be observed in Fig. 15 by comparing the average joint shear stresses in corresponding specimens with and without floor slabs; e.g., Specimens A1 and A4, and Specimens A2 and A3. Joint shear strength was increased at least 1.1 times by the floor slabs.

The enhancement is attributed to uniformly distributed shear stresses in the joint panel concrete, relieving the stress concentration from the joint diagonal compression strut, by shear from the slab concrete adjacent to the upper part of a joint in Specimen A4 without transverse beams, and by torsion of transverse beam framing into a joint in Specimen A3.

Note that the joint shear strength of Specimen A3 with both transverse beams and floor slabs, modeling the sub-assemblage of the actual frame structures, was more than 1.3 times larger than that of Specimen A1 without transverse beams nor floor slabs.

EFFECT OF COLUMN AXIAL LOAD ON BOND STRESS TRANSFER AND SHEAR

The relation of column compressive stresses normalized by the concrete compressive strength and equivalent viscous damping ratio h_{eq} at a story drift angle of 1/50 rad is shown in Fig. 18

for planar interior beam-column joint specimens tested in Japan to investigate the influence of column axial load on the bond stress transfer along the beam reinforcement in a joint. Solid circles represent specimen with beam bar bond index $u_b / \sqrt{f_c'}$ less than 4.5. Test results are scattered widely regardless of column axial stress level. Therefore, it is considered that column axial stress smaller than $0.3 f_c'$ does not exhibit beneficial effect on the bond resistance along the beam bar within a joint.

Column axial stress level is compared with the maximum joint shear stress normalized by concrete compressive strength for plane beam-column joint specimens, failed in joint shear, tested in Japan and U.S. (Fig . 19). Column axial load does not seem to influence the joint shear strength. High axial compression load in a column, however, accelerates the strength decay in the diagonal compression failure of the joint core concrete after beam flexural yielding.

LIMITATION OF INPUT SHEAR INTO JOINT

After bond deteriorated along the beam reinforcement within a joint, the joint shear must be resisted by the diagonal strut mechanism. The shear compression failure of the diagonal strut may be delayed by restricting a shear stress level and by providing nominal amount of lateral reinforcement.

The joint lateral reinforcement ratio is compared with value $u_b / \sqrt{f_c'}$ for plane beam-column joint specimens larger than the half scale, tested in Japan and U.S. (Fig . 20), in which v_u is the maximum joint shear stress observed in a test. The lateral reinforcement ratio was defined as the total cross-sectional area of joint lateral reinforcement divided by the column width and the distance of (7/8)d, where d is effective depth at the beam critical section. Note that the joint shear stress must be limited at given in Eq. (4) to prevent shear failure after beam flexural yielding;

$$\frac{v_u}{f_c'} \leq 0.25 \qquad (4)$$

The shear failure in a joint occurred at a story drift angle greater than 1/25 rad regardless of the amount of lateral reinforcement if the input shear stress v_u is greater than $0.25 f_c'$. On the contrary, the lateral reinforcement ratio of 0.27 % was sufficient to prevent shear failure when v_u is less than $0.25 f_c'$. From these test results and those of Specimen B1 with lateral reinforcement of 0.33%, minimum lateral reinforcement ratio of 0.35% is recommended. The required lateral reinforcement ratio of 0.4 % may be reduced if the joint shear stress is sufficiently lower than $0.25 f_c'$.

The shear strength of interior beam-column joints to with cracked transverse beam and slabs increased to 1.3 times more than that without transverse beams nor slabs. Therefore, the nominal shear strength of a joint may be enhanced up to 1.3 times required by Eq.(4); i.e., 0.33 f_c', if beams frame into four vertical faces of the joint and if at least two-thirds of each joint face is covered by framing beams.

CONCLUDING REMARKS

The earthquake response of R/C frame structures indicated that the member response amplitudes were not appreciably affected by hysteretic energy dissipation capacity at the beam ends. Therefore, beam bar bond deterioration should be tolerated in the interior beam-column joint. Consequently, joint shear must be resisted by the diagonal compression strut. Joint shear compression failure can be delayed by limiting joint shear stress level and providing nominal joint lateral reinforcement. The joint shear resistance is enhanced by the transverse beams and slabs.

Design provisions were suggested in order to maintain the building performance to a story drift angle of 1/50 rad, or to a beam ductility factor of 4.

(a) The ratio of the column width to the beam bar diameter must be limited as given in Eq. (3);

$$\frac{h_c}{d_b} \geq \frac{f_y}{9\sqrt{f_c'}} \qquad (3)$$

where, f_y: yield strength of beam bars in kgf/cm^2, d_b: diameter of beam bars, h_c: column width and f_c': concrete compressive strength in kgf/cm^2.

(b) The joint shear stress v_u must be limited as follows;

$$\frac{v_u}{f_c'} \leq 0.25 \qquad (4)$$

(c) A minimum lateral reinforcement ratio of 0.4 % is recommended. This required value may be reduced if the joint shear stress is sufficiently lower than 0.25 f_c'.

(d) The nominal shear strength of a joint may be enhanced up to 1.3 times required by Eq. (4); i.e., 0.33 f_c', if beams frame into four vertical faces of the joint and if at least two-thirds of each joint face is covered by framing beams.

(e) Column axial stress smaller than $0.3 f_c'$ does not exhibit beneficial effect on the bond resistance along the beam reinforcement within a joint, and the column axial stress smaller than $0.5 f_c'$ does not influence the joint shear strength.

REFERENCES

1. Standard Association of New Zealand, New Zealand Standard Code of Practice for the Design of Concrete Structures, NZS 3101, 1982.

2. American Concrete Institute, Building Code Requirements for Reinforced Concrete (ACI 318-83), 1983.

3. Paulay, T., R. Park, and M. J. N. Priestley, "Reinforced Concrete Beam-Column Joints Under Seismic Actions," Journal, American Concrete Institute, Vol. 75, 1978, pp. 585 - 593.

4. Kobayashi, Y., S. Otani, M. Tamari and H. Aoyama, "Experimental Study of Reinforced Concrete Sub-assemblages (in Japanese)," Japan Concrete Institute, 6th Conference, 1984, pp. 653 - 656.

5. Kitayama, K., K. Kurusu, S. Otani and H. Aoyama, "Behavior of Beam-Column Connections with Improved Beam Reinforcement Bond," Transactions, Japan Concrete Institute, Vol. 7, 1985, pp. 551 - 558.

6. Kitayama, K., and H. Aoyama, "Earthquake Resistance of Reinforced Concrete Beam-Column Sub-assemblages (in Japanese)," Proceedings, Seventh Japan Earthquake Engineering Symposium, 1986, pp. 1687 - 1692.

7. Kitayama, K., S. Otani and H. Aoyama, "Research on Role of Lateral Reinforcement within R/C Interior Beam-Column Connections (in Japanese)," Architectural Institute of Japan, Summaries of Technical Papers of Annual Meeting, Vol. C, 1988, pp. 423 -424 .

8. Kitayama, K, C. Kojima, S. Otani and H. Aoyama, "Behavior of Reinforced Concrete Interior Beam-Column Joint subjected to High Shear (in Japanese)," Proceedings, Japan Concrete Institute, Vol. 11, 1989, pp. 531 - 536.

Table 1: Properties of Specimens J1, C1, B1,B2 and B3

Specimen	J1	C1	B1 / B2	B3
(a) Beam (200x300 mm)				
Top Bars	8-D13	12-D10	8-D13	12-D10
a_t (mm^2)	1016	856	1016	856
p_t (%)	1.88	1.59	2.05	1.68
Bot. Bars	4-D13	6-D10	8-D13	12-D10
a_t (mm^2)	508	429	1016	856
p_t (%)	0.94	0.79	2.05	1.68
f_y (kgf/cm^2)	4090	3260	3780	3170
Stirrups	2-D6	2-D6	2-R6	2-R6
@ (mm)	50	50	50	50
p_w (%)	0.64	0.64	0.56	0.56
f_y (kgf/cm^2)	3750	3300	4980	4980
(b) Column (300x300 mm)				
Total Bars	16-D13	16-D13	16-D16	16-D13
a_g (mm^2)	2032	2032	3184	2032
p_g (%)	2.26	2.26	3.54	2.26
f_y (kgf/cm^2)	4090	4300	3580	3780
Hoops	2-D6	4-D6	4-R6	2-R6
@ (mm)	80	50	50	50
p_w (%)	0.27	0.85	0.75	0.37
fy (kgf/cm^2)	3750	3300	4980	4980
Axal Load (tonf)	18.0	18.0	18.0	18.0
Stress (kgf/cm^2)	20.0	20.0	20.0	20.0
(c) Connection				
Hoops	2-D6	2-D6	2-R6	3-R6
sets	3	3	4	7
a_w (mm^2)	192	192	225	592
p_w (%)	0.27	0.27	0.35	0.88
Shape	closed	closed	leg/closed	leg
f_y (kgf/cm^2)	3750	3300	2400	2400
f_c (kgf/cm^2)	262	261	250	250
f_t (kgf/cm^2)	25	25	26	26
BI index	5.35	3.21	5.20	3.33

Note: a_t : total area of tensile reinforcement, p_t : tensile reinforcement ratio,
a_g : total area of longitudinal reinforcement,
p_g : gross reinforcement ratio,
a_w : total area of web reinforcement placed between top and bottom beam bars,
p_w : web reinforcement ratio, f_y : yield strength,
f_c : concrete compressive strength, f_t : concrete tensile strength,
BI index: defined by Eq.(1).

Table 2: Properties of Buildings for Analysis

	Height (m)	Weight (tonf)	Fundamenal Period(sec.) (1)	(2)	Base Shear Coefficient
4-story	14.0	140	0.28	0.36	0.30
7-story	25.0	247	0.50	0.62	0.28
16-story	56.0	642	1.12	0.98	0.22

Note (1): periods calculated by 0.02h (sec), where h: height (m).
(2): periods calculated by accurate analysis

Table 3: Member Dimensions (Unit: mm)

(a) 4-story building

Story	Beam	Story	Column
RF - 2F	400x700	4F - 1F	700x700

(b) 7-story building

Story	Beam	Story	Column
RF - 6F	350x650	7F - 6F	750x750
5F - 2F	400x700	5F - 4F	750x750
		3F - 1F	800x800

(c) 16-story building

Story	Beam	Story	Column
RF - 15F	400x700	16F - 11F	700x700
14F - 12F	500x800	10F - 6F	800x800
6F - 2F	600x850		

Table 4: Properties of A-Series Specimens

Specimen	A1	A2	A3	A4
a) Longitudinal Beam				
Top Bars	8-D13	8-D13	6-D13	6-D13
at (cm^2)	10.16	10.16	7.62	7.62
p_t (%)	2.05	2.05	1.54	1.54
Bottom Bars	4-D13	4-D13	4-D13	4-D13
a_t (cm^2)	5.08	5.08	5.08	5.08
p_t (%)	0.96	0.96	0.96	0.96
Stirrups	4-D6	4-D6	4-D6	4-D6
@ (cm)	4.0	4.0	4.0	4.0
p_w (%)	1.6	1.6	1.6	1.6
b) Transverse Beam	(none)			(none)
Top Bars		7-D13	4-D13	
a_t (cm^2)		8.89	5.08	
p_t (%)		1.91	1.09	
Bottom Bars		4-D13	4-D13	
a_t (cm^2)		5.08	5.08	
p_t (%)		1.02	1.02	
Stirrups		2-D6	2-D6	
@ (cm)		5.0	5.0	
p_w (%)		0.64	0.64	
c) Column (common)				
Total Bars	16-D16	16-D16	16-D16	16-D16
a_g (cm^2)	31.84	31.84	31.84	31.84
p_g (%)	3.54	3.54	3.54	3.54
Hoops	4-D6	4-D6	4-D6	4-D6
@ (cm)	4.0	4.0	4.0	4.0
p_w (%)	1.07	.1.07	1.07	1.07
Axial Load (tonf)	18.0	18.0	18.0	18.0
Stress (kgf/cm^2)	20.0	20.0	20.0	20.0
d) Connection (common)				
Hoops	3-R6	3-R6	3-R6	3-R6
sets @ (cm)	3@4.5	3@4.5	3@4.5	3@4.5
a_w (cm2)	2.55	2.55	2.55	2.55
p_{jh} (%)	0.38	0.38	0.38	0.38
e) Slab	(none)	(none)		
Longitudinal Dir.			24-D6	24-D6
@ (cm)			9.0	9.0
st. ratio(%)			0.42	0.42
Transverse Dir.			14-D6	14-D6
@ (cm)			15.0	15.0
st. ratio(%)			0.27	0.27

Table 5: Material Properties of A-Series Specimens

Concrete	(kgf/cm^2)		
Compressive Strength	312		
Tensile Strength	26		
Reinforcing Bars	**Yield Stress**	**Tensile Strength** (kgf/cm^2)	**Strain at Hardening**
R6 (Lateral Reinf. in Joint)	3260	4350	0.0254
D6 (Shear Reinf. in Beam and Column)	4300	5500	0.0105
D13 (Transverse Beam Bar)	3460	5300	0.0159
D13 (Longitudinal Beam Bar)	7950	8510	0.0269
D16 (Column Bar)			

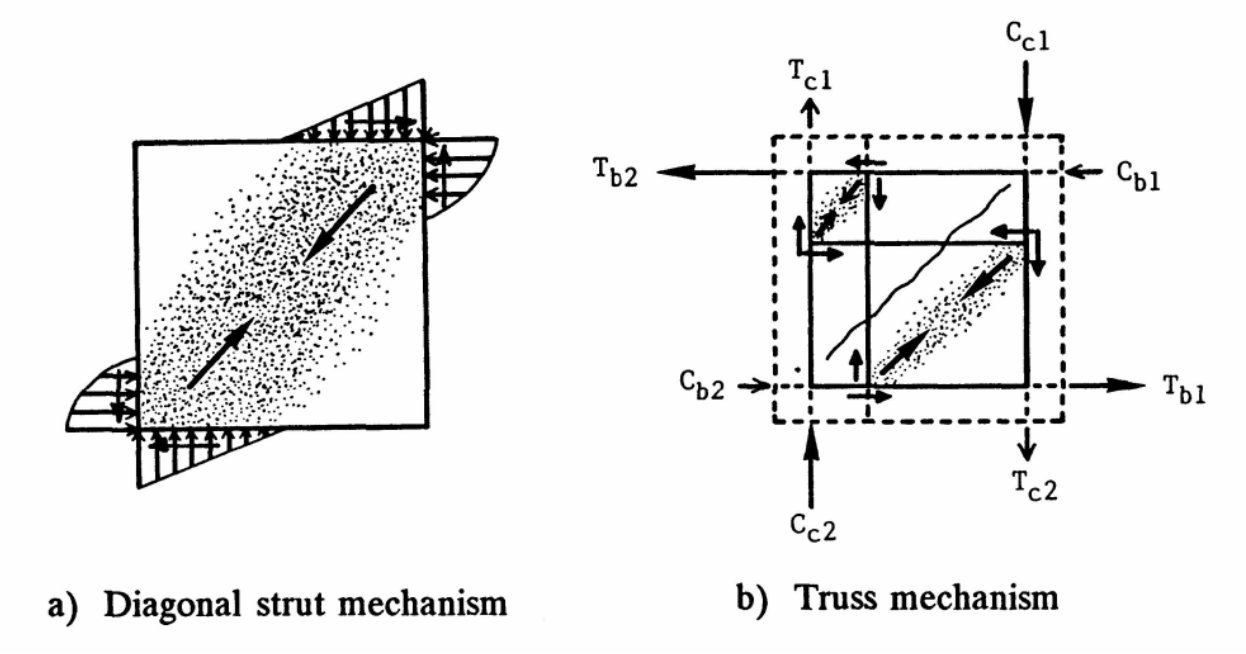

Fig. 1: Shear transfer mechanism in joint

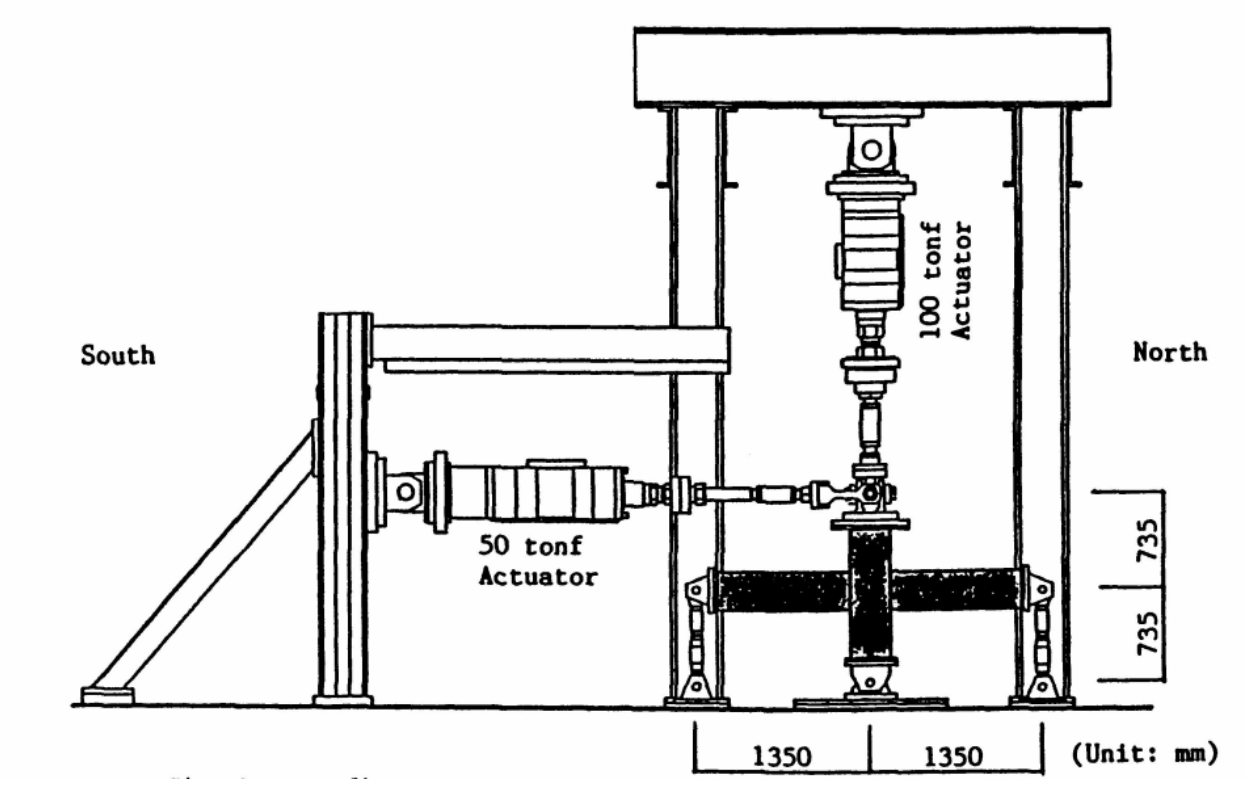

Fig. 2: Loading appratus

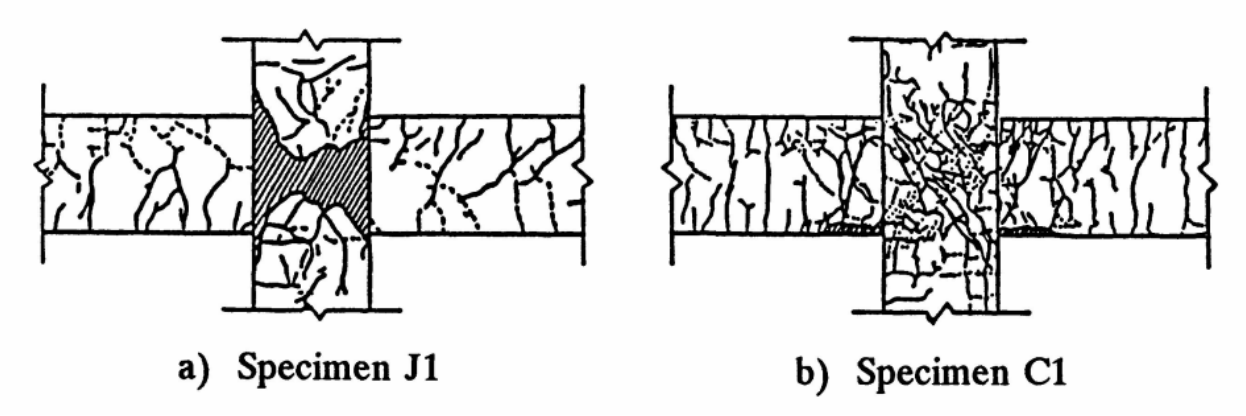

Fig. 3: Crack patterns of specimens J1 and C1

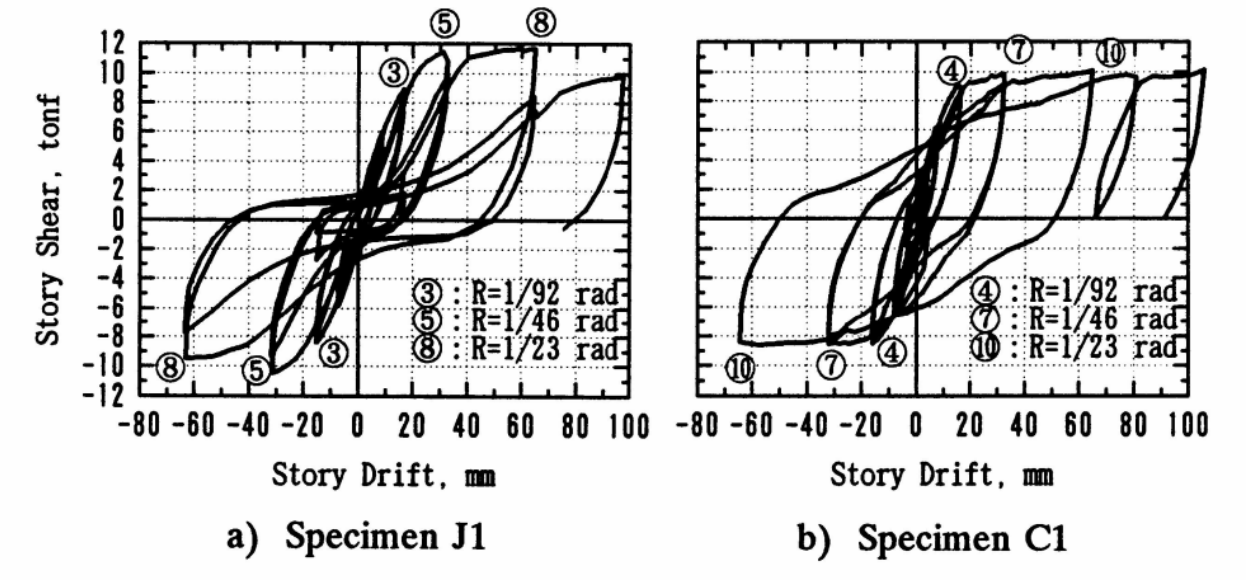

Fig. 4: Story shear-story drift relations of specimens J1 and C1

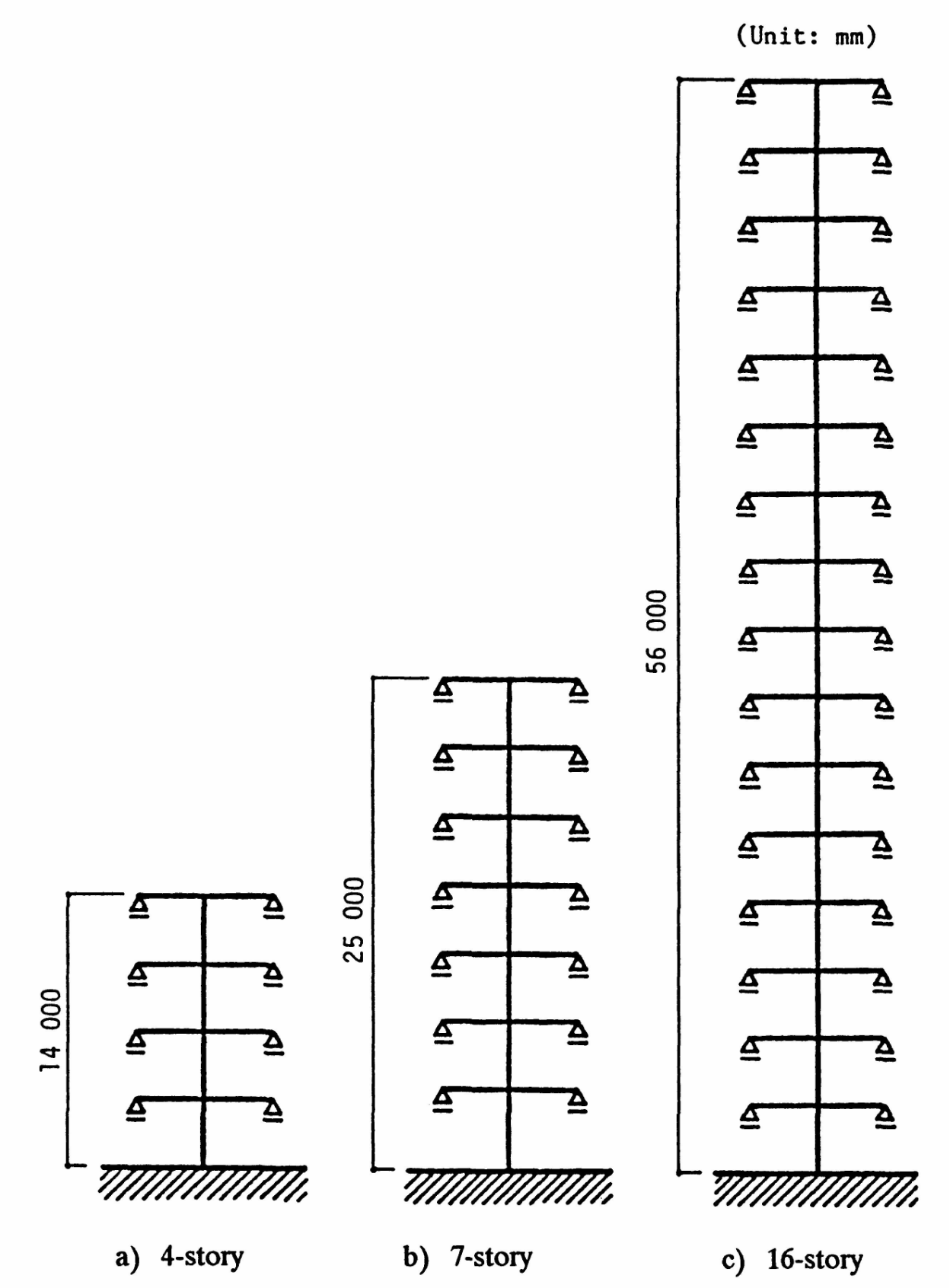

Fig. 5: Fish-bone models

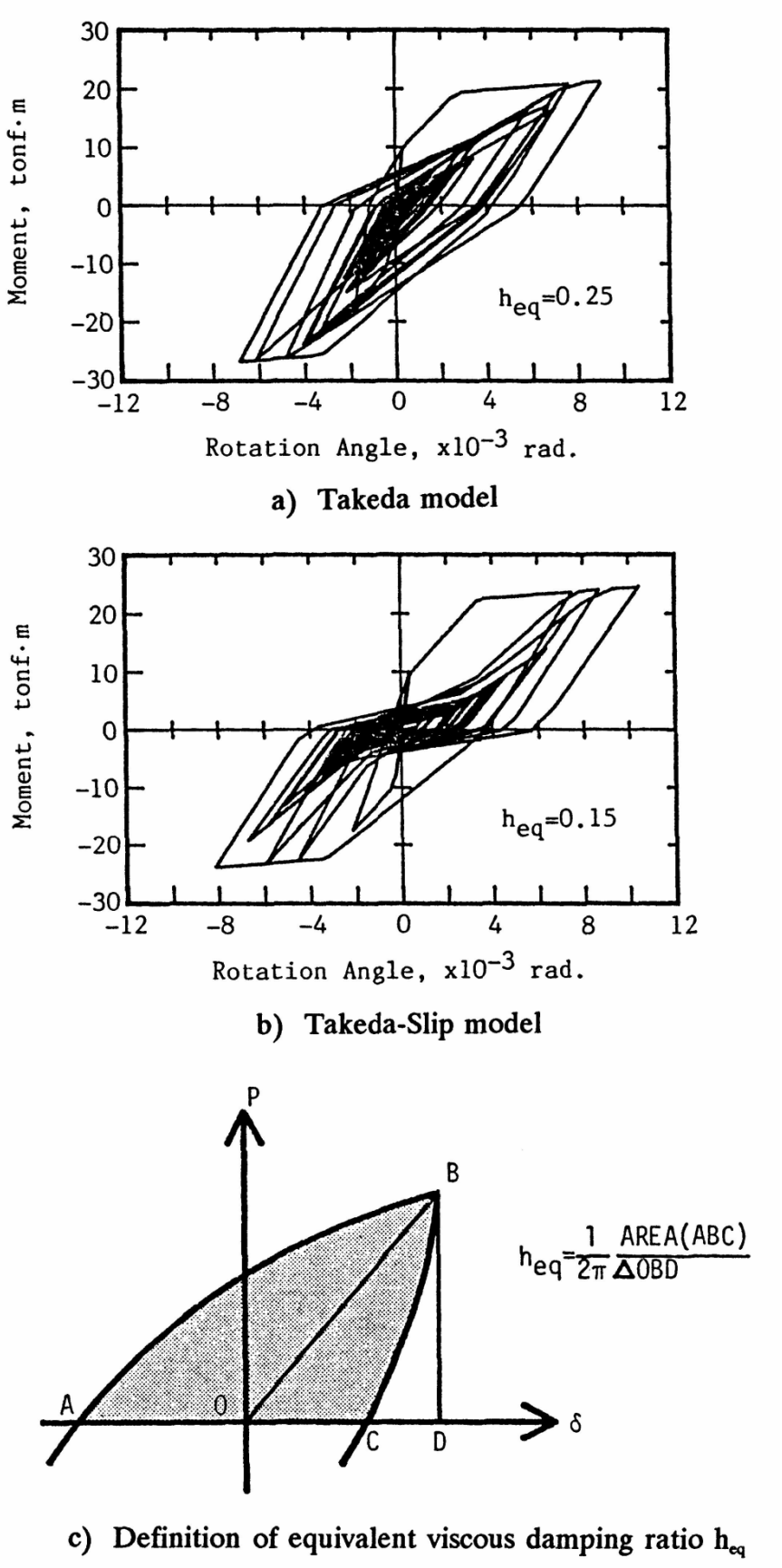

Fig. 6: Hysteresis models

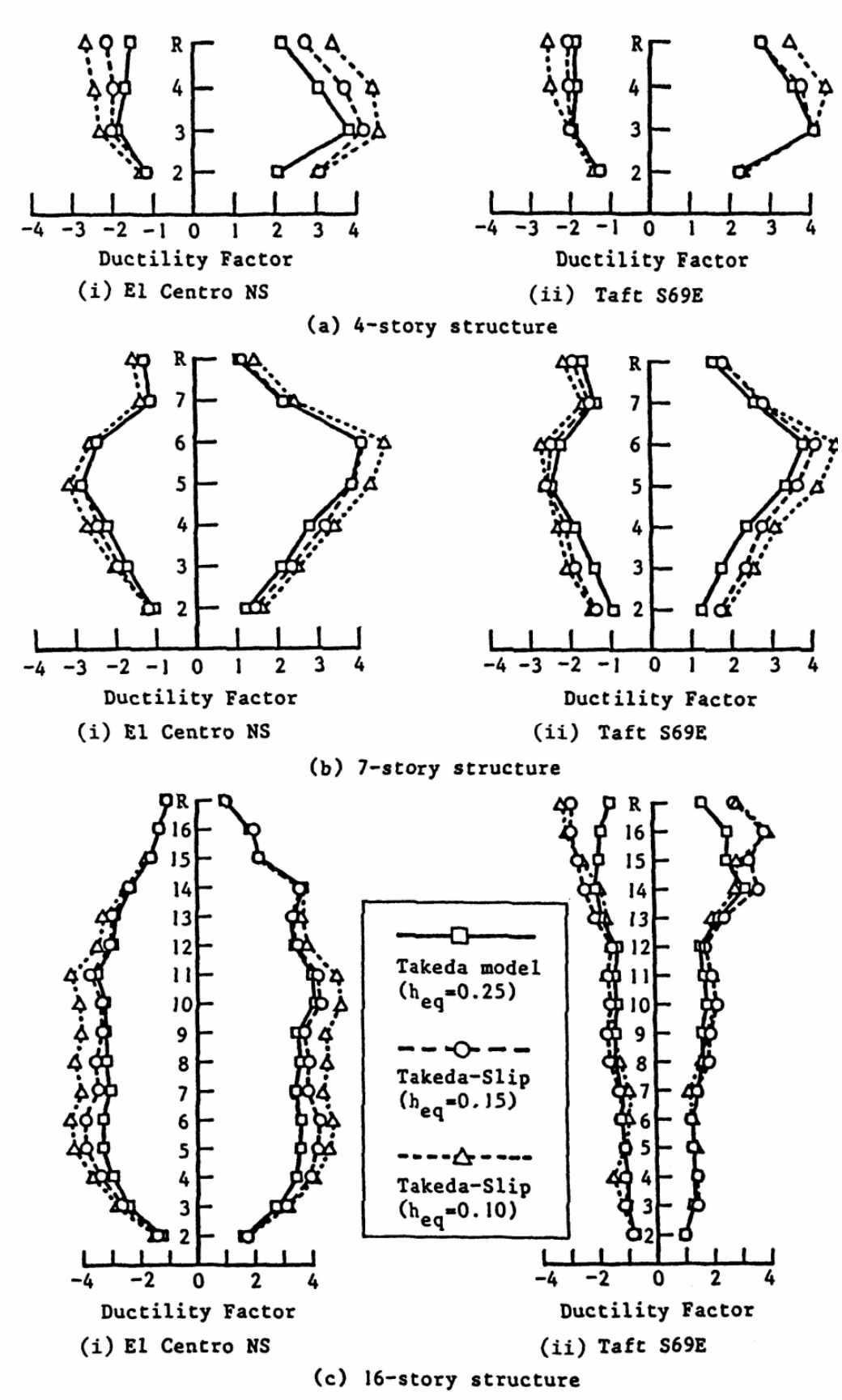

Fig. 7: Attained ductility factors at beam ends

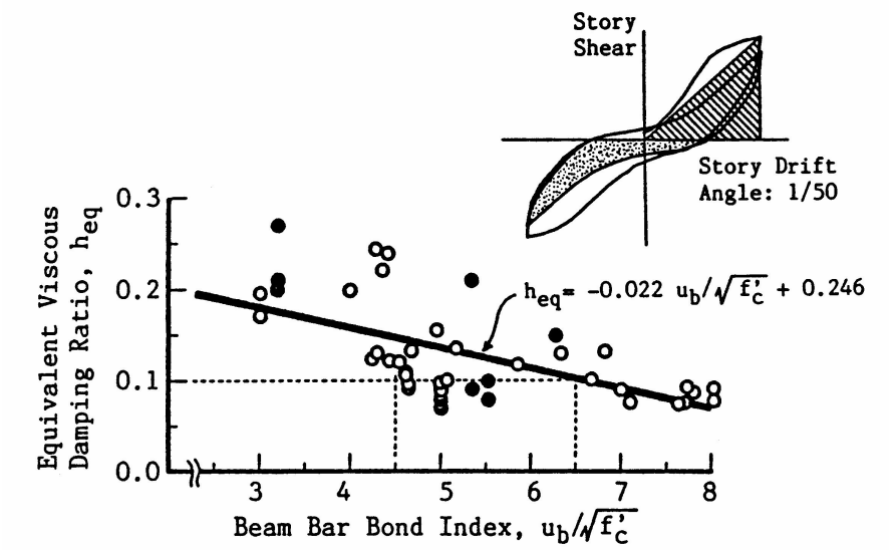

Fig. 8: Equivalent viscous damping ratio-beam bar bond index relation

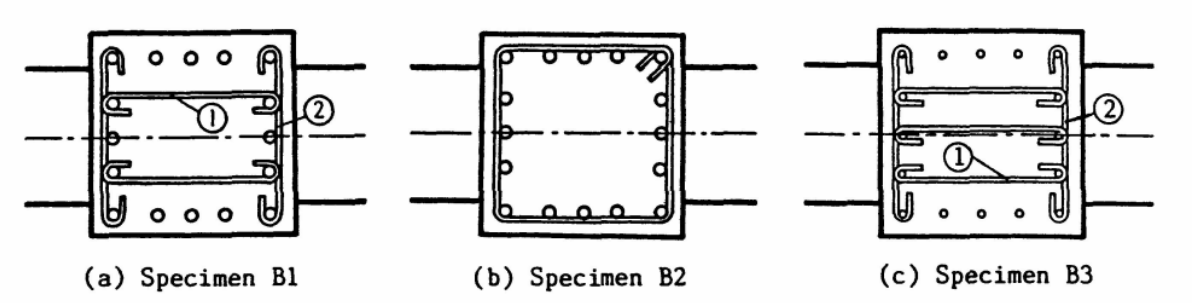

Fig. 9: Detail in joint lateral reinforcement

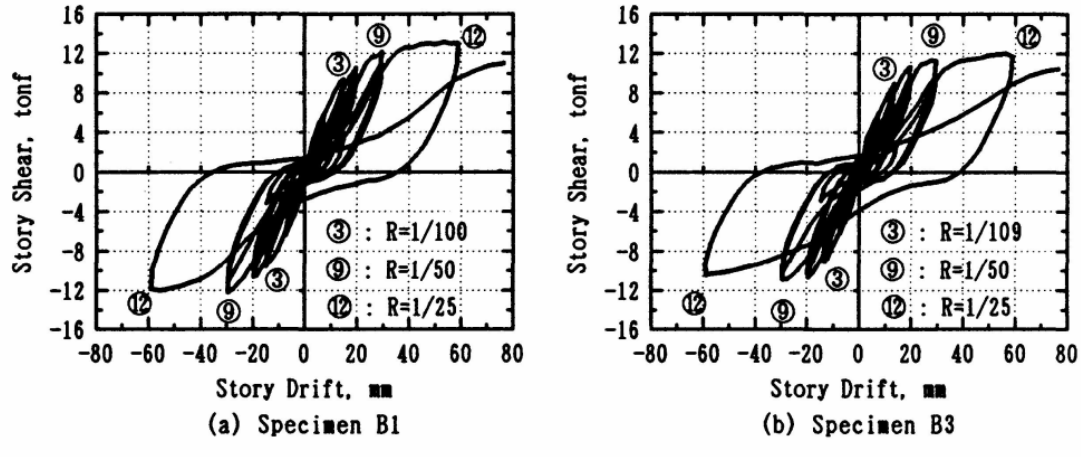

Fig. 10: Story shear-story drift relations

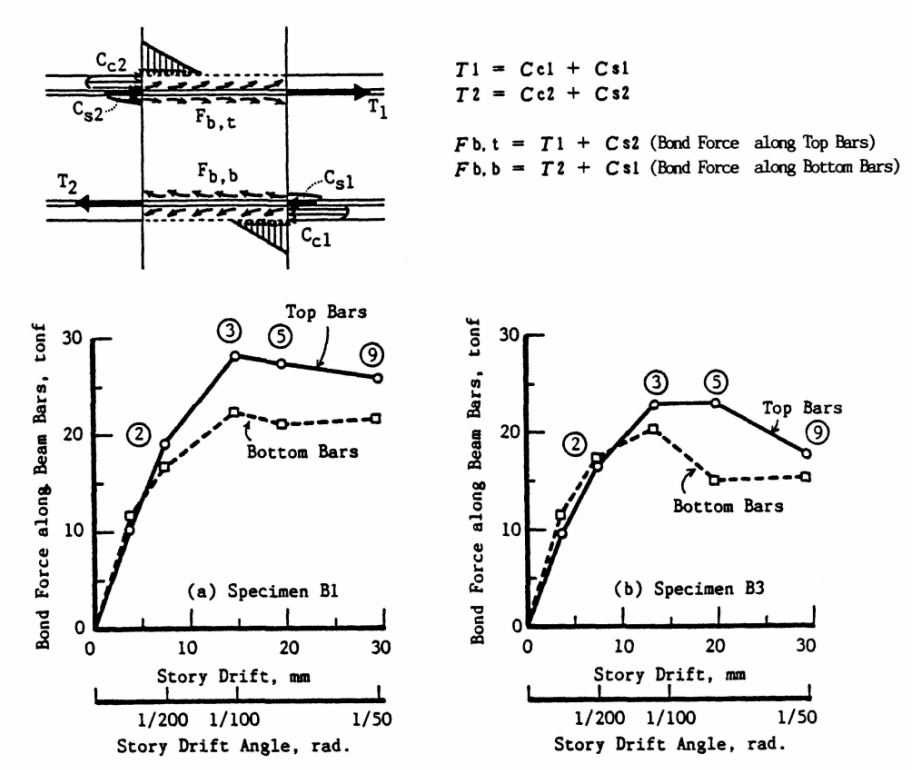

Fig. 11: Bond forces along beam bars within joint

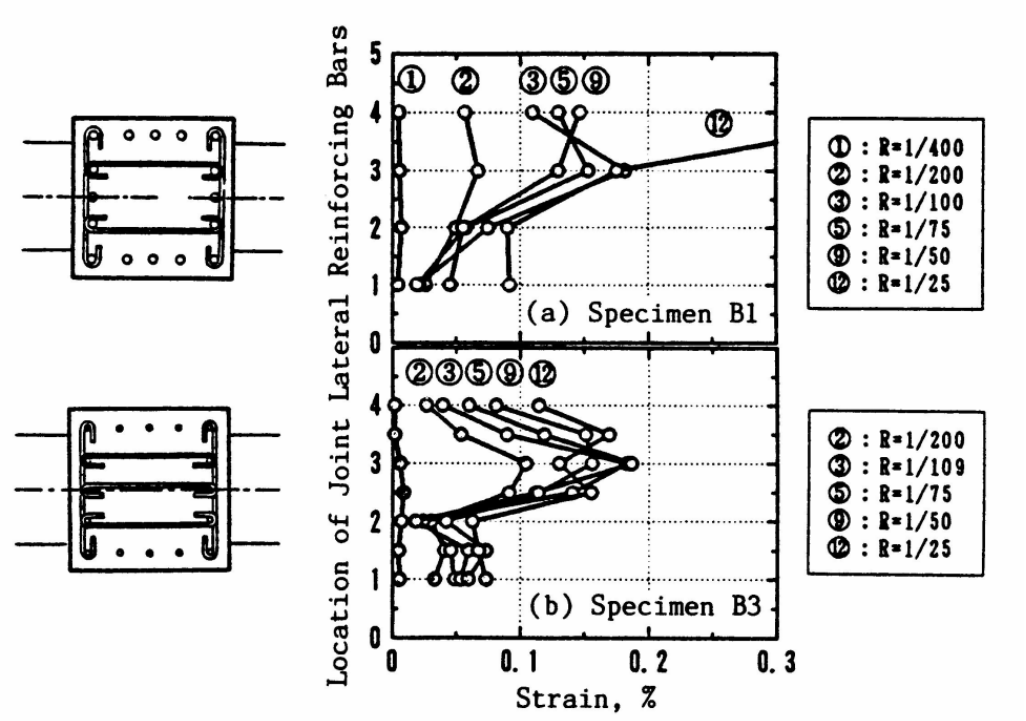

Fig. 12: strains in joint ties parallel to loading direction

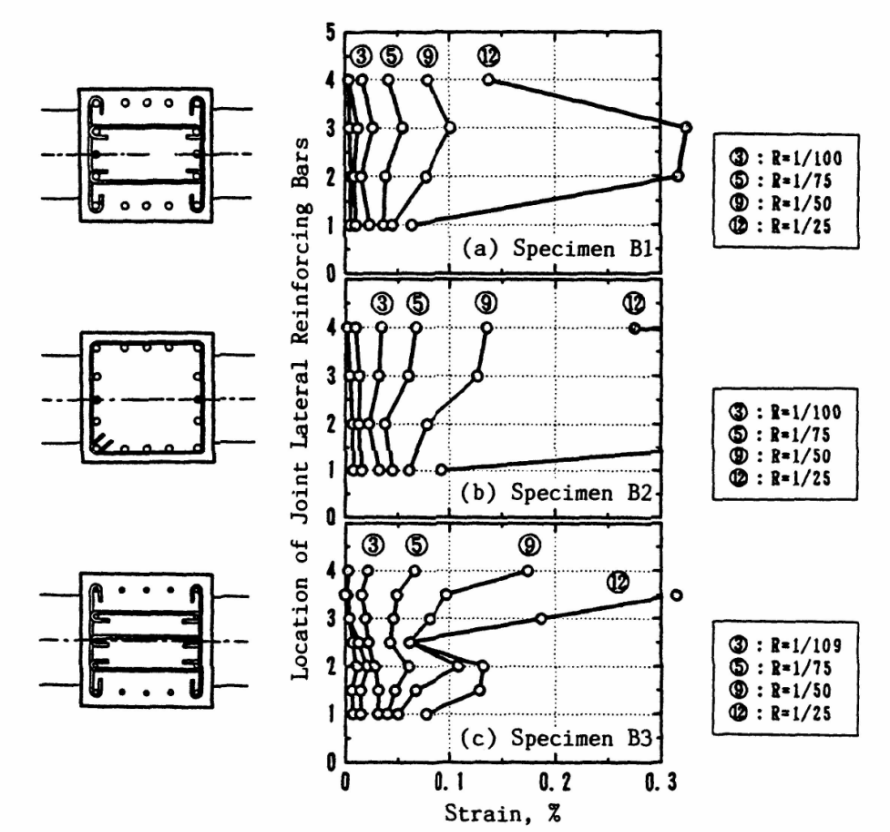

Fig. 13: Strains in joint ties orthoglanal to loading direction

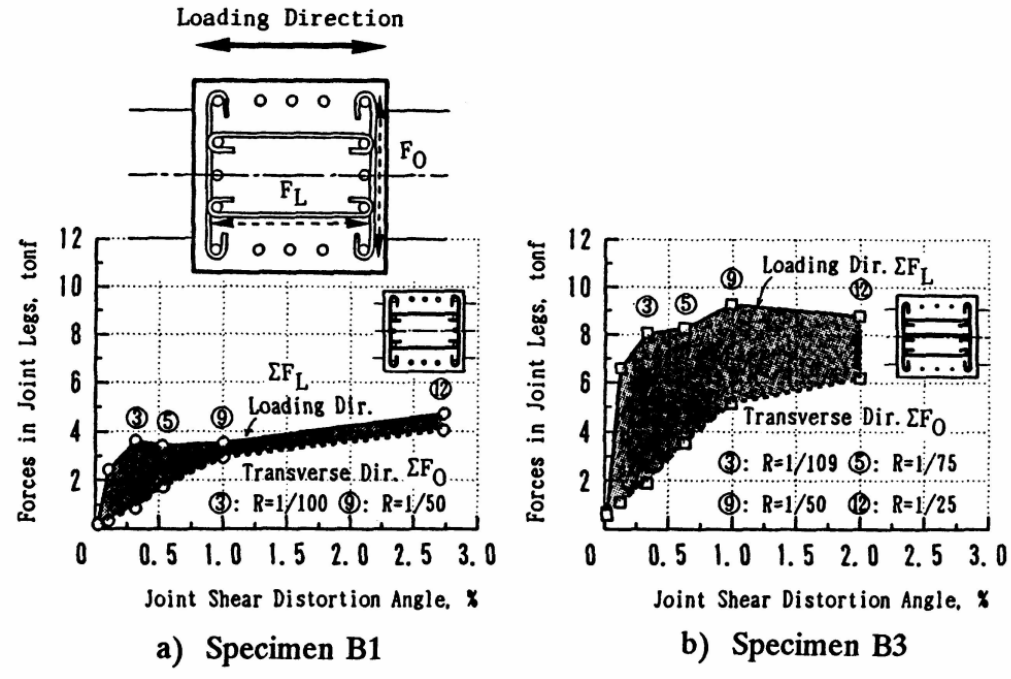

Fig. 14: Total tensile forces in joint ties

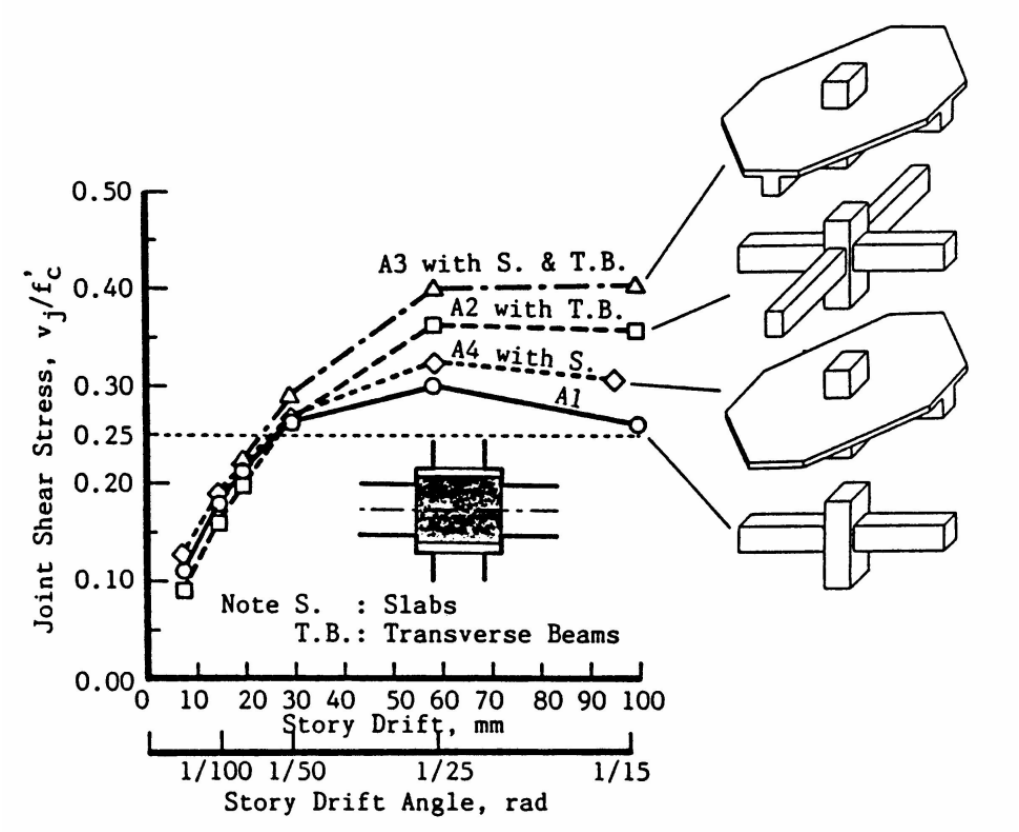

Fig. 15: Story drift-joint shear relations

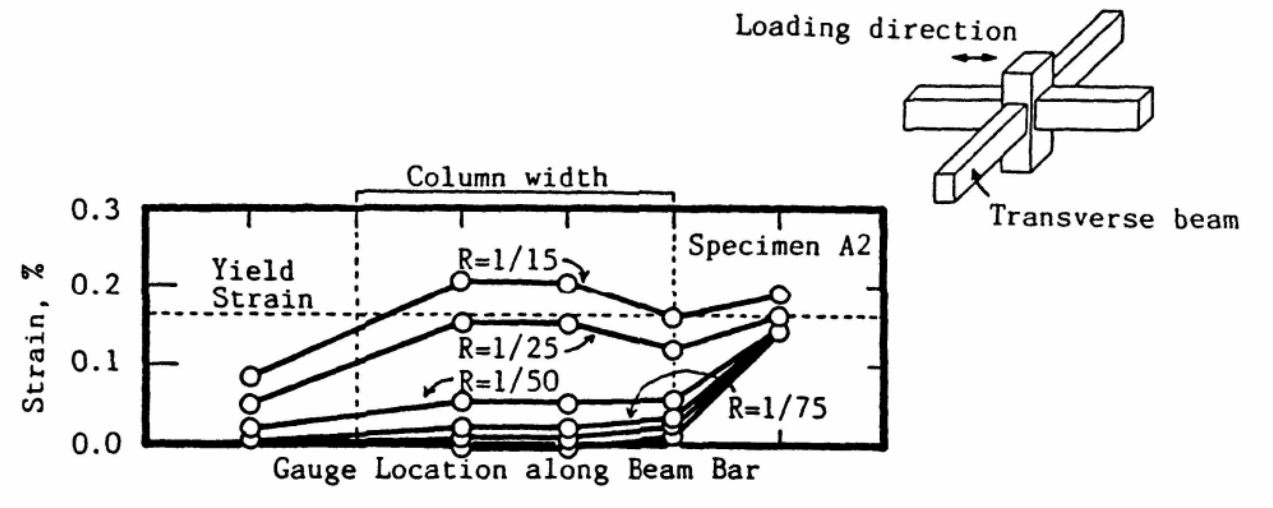

Fig. 16: Strains along transverse beam bar

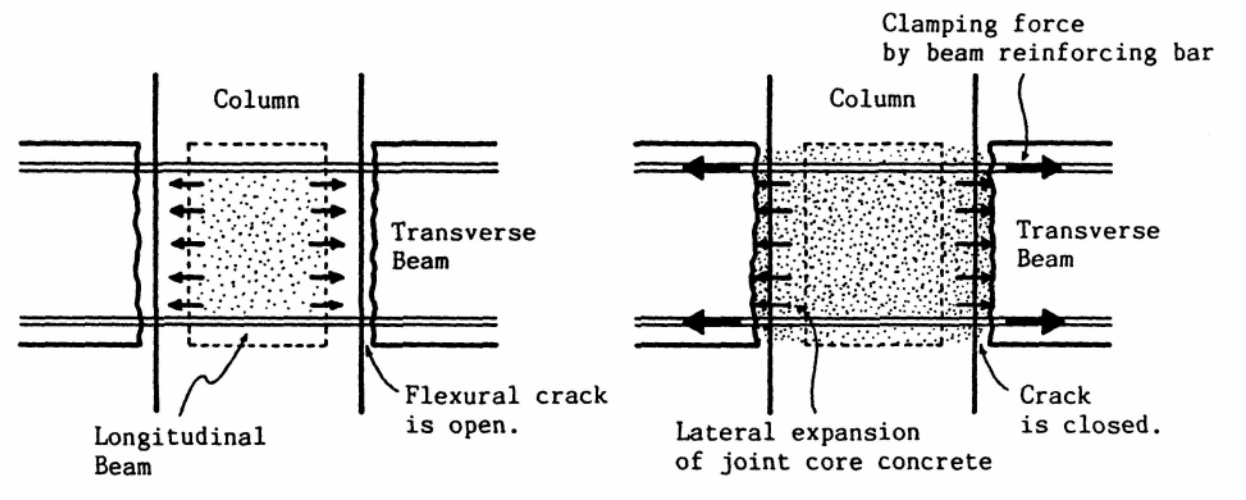

Fig. 17: confinement action due to cracked transverse beams

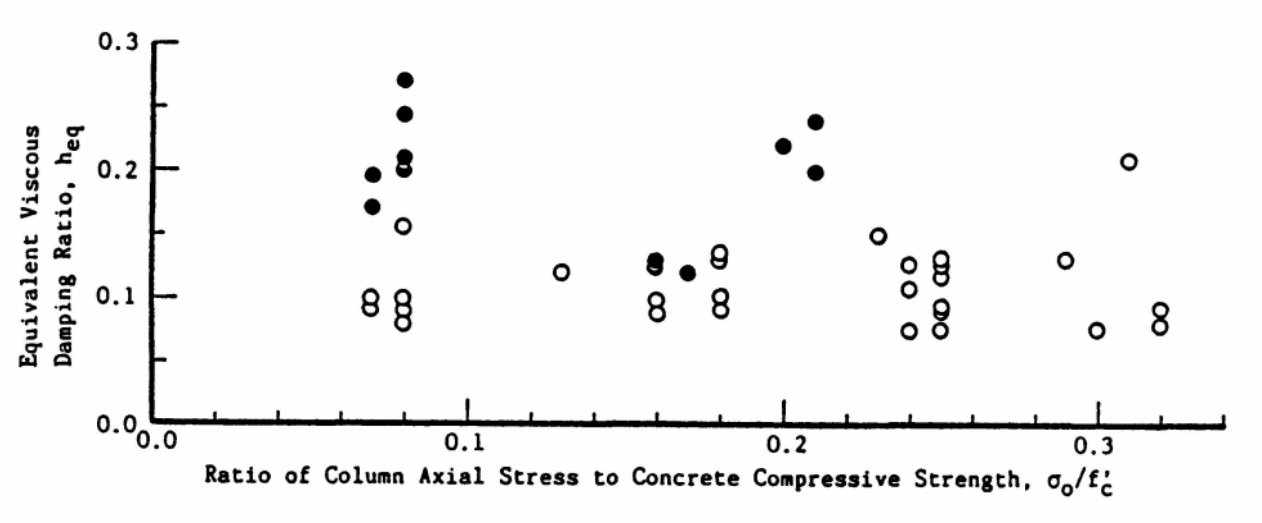

Fig. 18: Effect of column axial load on bond condition along beam reinforcement

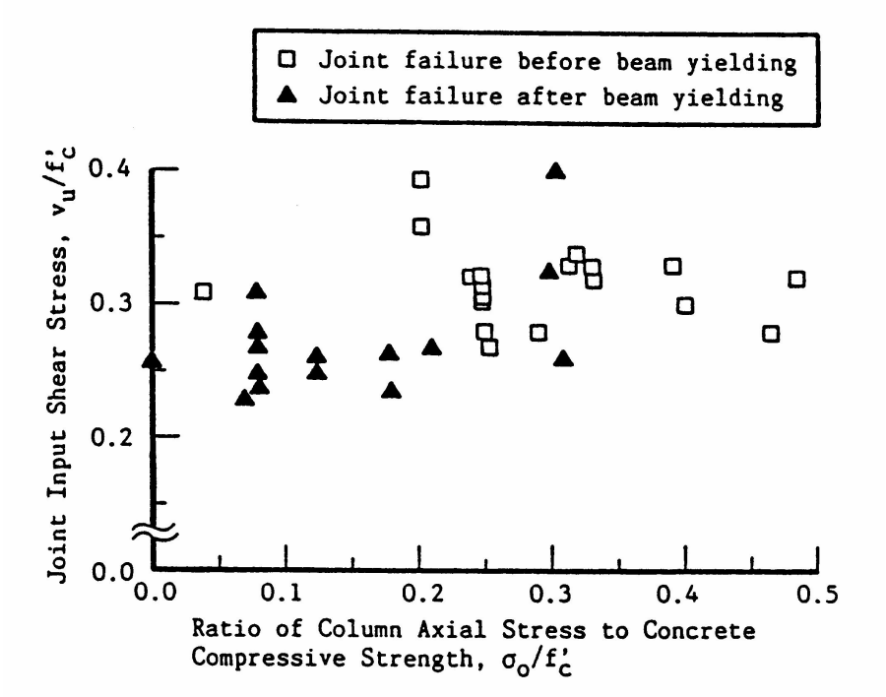

Fig. 19: Effect of column axial load on joint shear strength

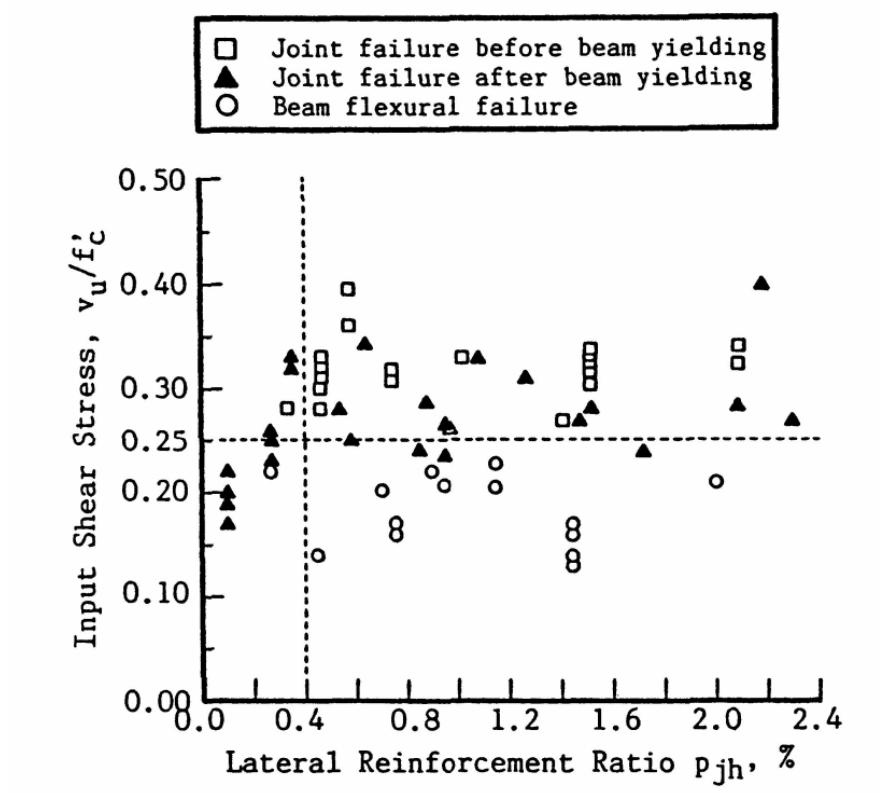

Fig. 20: Joint shear stress-joint lateral reinforcement ratio relation